J. Basic. Appl. Chem., 8(3)9-18, 2018

ISSN 2090-424X
Journal of Basic and Applied Chemistry
www.textroad.com

Open Circuit Potential and Potentiodynamic View on the Behavior of Different Four Electrodes in Artificial Saliva Solution for Usage in Dental Application

E. M. Attia*, R.M. Abou Shahba and F.M. Abou Koffa

Chemistry Department, Faculty of Science (Girls), Al-Azhar University, Nasr City, Cairo, Egypt.

ABSTRACT

This work aimed to study the corrosion behavior of CoCr-alloy, Nb and Mo electrodes compared with Au electrode in artificial saliva solution and the effect of changing the temperature; using open circuit and potentiodynamic techniques. The obtained results revealed that under open circuit conditions, the rest potential (E_{res}) values for each electrode became less noble with increasing temperature. The E_{res} for the different four electrodes decreased in artificial saliva solutions at all temperatures according to the following order: Au > CoCr-alloy > Mo > Nb.

Under potentiodynamic polarization measurements, Au, CoCr-alloy and Mo electrodes showed typical Tafel behavior at all temperatures. The niobium electrode exhibited a typical Tafel behavior in the cathodic region only at all temperatures. The corrosion rates (C_R) for all electrodes increased with increasing the temperature. The C_R values decreased tracking the following descending order at all temperatures: CoCr-alloy > Nb > Mo > Au. The difference recorded between corrosion rates of Mo, Nb and CoCr-alloy compared with that of Au electrode reached its minimum values in Mo electrode. Activation energy (E_a), enthalpy (ΔH) and entropy (ΔS) of dissolution were calculated and discussed.

KEYWORDS: CoCr-alloy, Au, Mo, Nb, Artificial saliva, Open circuit, Potentiodynamic.

INTRODUCTION

Some metals and alloys used in dental application react easily with the biochemical medium in the oral cavity and respond simply to electrochemical corrosion. From electrochemical point of view, the selection of dental metals and alloys are corrosion resistance dependence on these materials. They must resist the corrosion caused by solutions inter into the mouth.

Saliva is the natural biochemical solution contained in the mouth. Its normal pH is slightly alkaline (7.4) [1]. It is an excellent buffer for the entire mouth, as it is saturated with ions which constitute the mineral content of the teeth [2]. The famous electrolytes constituting saliva include sodium, potassium, calcium, magnesium, bicarbonate, chloride and phosphate [3]. The artificial alternatives of saliva act as a replacement of the mucoadhesive, lubricative and protective function of the natural saliva. Many authors studied the behavior of metals and alloys used in dental application in artificial saliva solutions [1, 4-6]. Karthega *et al*. [7] reported that Ti-6Al-4V alloy shows an improved corrosion resistance in artificial saliva containing 1% NaF at pH 7.0. A wide study was performed by Renita *et al*. [8] who discovered that the existence of chloride ions in the saliva solutions causes pitting corrosion. In the contrary, the corrosion resistance increases by adjusting the acidity of saliva to pH 4 and by feeding saliva with high protein content.

This research aimed to investigate the behaviors of CoCr-alloy, Nb and Mo electrodes compared with Au electrode in artificial saliva solution, so as to be used as alternatives of gold in dental applications. The study was performed using open circuit potential and potentiodynamic polarization techniques at temperature range 20 - 50°C.

2. MATERIALS AND METHODS

2.1. Electrode preparation

Massive cylindrical spectroscopically pure niobium supplied by Johnson Matthey- England, and molybdenum rod supplied by Aldrich – Chemie were used as working electrodes. A commercial sample of CoCr-alloy (WIRONITR, BEGO, Germany) had the following composition: 64% Co, 28% Cr, 6% Mo, 2% (C + Si + Mn) was also used. Gold electrode of chemical composition: 98.2% Au, 1.7% Ti and 0.1% Ir, was used as a blank electrode.

Corresponding Author: E. M. Attia, Chemistry Department, Faculty of Science (Girls), Al-Azhar University, Nasr City, Cairo, Egypt.

Each electrode was mounted in a glass tube of appropriate diameter leaving a specified circular surface area (0.33, 0.196, 1.038 and 0.0184 cm² for niobium, molybdenum, CoCr-alloy and gold electrodes respectively) to contact the electrolyte. The surfaces of electrodes were mechanically polished via a standard procedure with emery papers of increasing grit: 320, 600, 800, 1000, 1500 and 2000. After polishing, the electrodes were thoroughly rinsed with bi-distilled water, degreased in ethanol for about 20 sec (to remove the greasy particles) and then again rinsed with bi-distilled water. The electrodes surfaces were finally wrapped against a soft cloth, washed with triply distilled water, and then immersed quickly in the test solution.

2.2. Solution:

Tested solution was prepared from analytical reagent grade according to Ringer's solution (type of artificial saliva) [9]. The solution typically contains 9g NaCl + 0.24g $CaCl_2$ + 0.43g KCl + 0.2g $NaHCO_3$ all dissolved in 1 L of water [10].

2.3. Experimental techniques

2.3.1. Open circuit potential measurements

Open circuit potential (OCP) measurements were carried out in a double- walled glass cell filled with 25 mL of the test solution. The potentials *vs.* time were performed with digital multimeter (KEITHLEY, Model 175, USA) using saturated calomel electrode (SCE) as a reference electrode.

2.3.2. Potentiodynamic polarization measurements

Potentiodynamic polarization measurements were generated using an Electronic Potentioscan Wenking (Model POS 73). A saturated calomel electrode (SCE) and a platinum sheet (4 cm²) were used as the reference and auxiliary electrodes, respectively. The working electrodes were polarized by submission to a potentiodynamic scan from -5 to +5 V/SCE at scan rate of 3.33 mV/s and the corresponding currents were recorded. The potentiodynamic curves were recorded after the electrodes were immersed in the test solution for 90 min in order to reach a steady-state OCP value, followed by the polarization measurement. Values of corrosion current (I_{corr}) and corrosion potential (E_{corr}) were evaluated from intersection of the linear anodic and cathodic branches of Tafel plots. Each experiment was repeated at least three times at each studied temperature. The corrosion rate (C_R) in mpy, was calculated using Eq.1 [11]:

$$C_R = 0.13 \times I_{corr} \times e/d \quad \ldots\ldots\ldots\ldots\ldots\ldots (1)$$

where 0.13 is the metric and time conversion factor, I_{corr}, is the corrosion current density in µA/cm², e and d are the equivalent weight and density of metal in geq/mol and g/cm³ respectively.

3. RESULTS AND DISCUSSION

3.1. Open circuit potential measurements

The variation of open circuit potentials with exposure time of the different four electrodes (namely CoCr-alloy, Nb, Mo and Au) in artificial saliva solution, for a period of 90 min at the temperature range 20 – 50°C were studied. Figure 1 illustrates the behavior of the tested electrodes at 20°C.

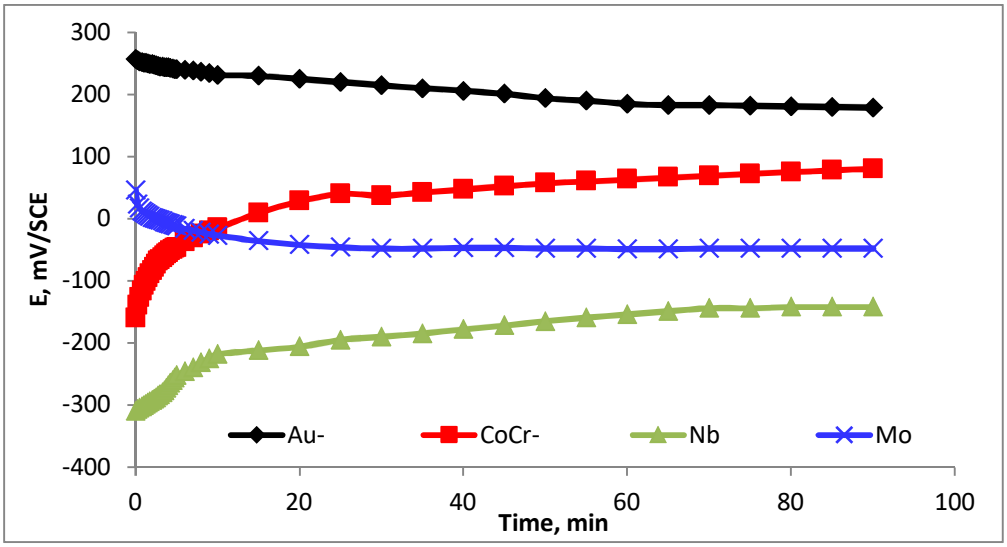

Figure 1: Potential – time curves of the four studied electrodes in artificial saliva solution at 20°C.

The plot illustrates that; curves of Au and Mo electrodes move downwards, i.e. the potential decreases gradually during the early stage of immersion, and then stabilize with further increasing immersion time. On the other hand the potentials increase rapidly in the first 10 minutes in case of CoCr-alloy and Nb electrodes. This indicates increasing the rate of oxide thickening parallel to increasing the potential. This stage represents the formation of films actually responsible for protection of the metals. The same behavior was observed at 30, 40 and 50°C for all studied electrodes.

Although the first 10 minutes of immersion represent dissolution process for Au and Mo electrodes and passivation process for CoCr-alloy and Nb electrodes; it is observed that the Au electrode has the highest potential values for all the immersion period indicating the best protection properties of all electrodes. Concerning the behavior of Mo electrode, the plot illustrates that Mo has higher potential values than CoCr-alloy in the first 7 minutes of immersion, and has higher potential values than Nb electrode for all the immersion period. Instead, Nb electrode provides the lowest potential values for all electrodes. The immersion potential (E_{imm}) and rest potential (E_{res}) for all electrodes at all studied temperatures are recorded in Table 1.

Table 1 illustrated that Nb had the most negative E_{res} values at all studied temperatures. For each electrode, E_{res} becomes less noble with increasing temperature. The rest potentials for the different electrodes decreased in artificial saliva solutions at all temperatures according to the following order: Au > CoCr-alloy > Mo > Nb

The anodic oxidation in aqueous solutions for the classic niobium valve metal follows the familiar relationship [12]:

$$I_a = A \exp(BH) \qquad \text{……..(2)}$$

Where, I_a is the imposed anodic current density, A and B are constants, and H is the effective field strength.

Abd El– Kader and Shams El– Din [13] suggested that, under open- circuit conditions, the adsorbed anions on the oxide covered metal could originate anodic current, I_a. This made the oxide/metal interface oppositely charged with charges of the same magnitudes that stimulate transfer of ions through the oxide. It was further suggested that H in Equation (2) could be recognized as E/δ, where E is the measured electrode potential corresponding to a saturated calomel electrode, and δ is the oxide film thickness.

The transformation of electrode potentials towards positive values, as illustrated by CoCr-alloy and Nb electrodes in Figure 1, go along with corresponding increase in the oxide film thickness, in order to keep the field strength (E/δ) constant. Therefore the equation, which describe the variation of the electrode potential (|E|) with the time for metals carrying thin oxide films can be represented by:

$$|E| = ɖ + 2.303\ (\delta/\beta)\ \log t \qquad \text{…….……..(3)}$$

Where ɖ is a constant and δ represents the rate of oxide thickening per unit decade of time. The term β is identified as:

$$\beta = \frac{nF}{RT}\ \alpha\ \delta` \qquad \text{……..….(4)}$$

Where α is the charge transference coefficient encountered in normal electrochemical processes ($0 < \alpha < 1$) and $\delta`$ is the height of the energy barrier surmounted during charge transfer [14].

Figure 2 illustrates a graphical representation of equation 3. From the slopes of the straight lines, the rate of oxide thickening were calculated and recorded in Table 1.

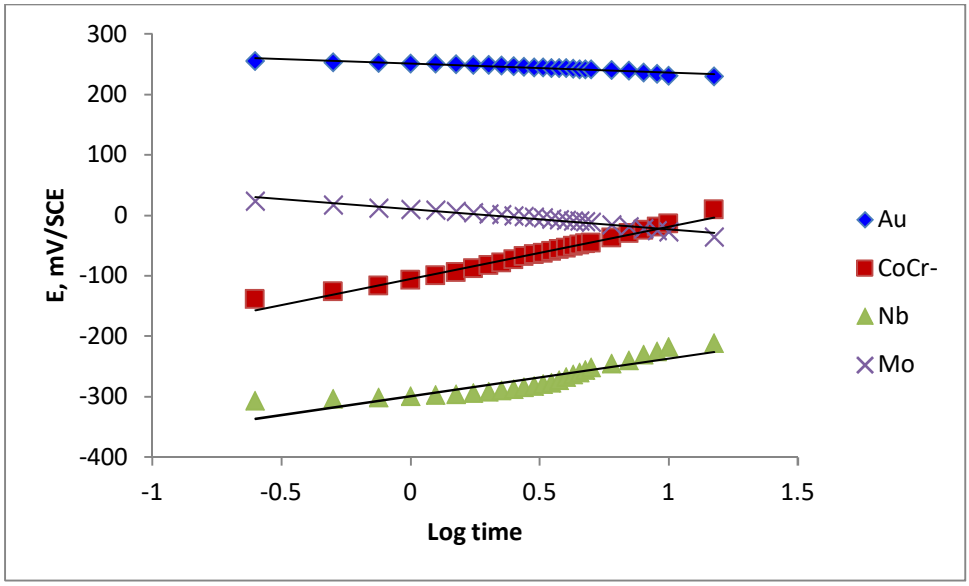

Figure 2: E –Log t plot of tested electrodes in artificial saliva solutions at 20°C.

Table 1: Immersion (E_{imm}) and rest (E_{res}) potentials, slopes of the linear parts, rates of oxide film thickening (δ) and regression coefficient (R^2) of tested electrodes, at temperature ranges 20 – 50°C

Electrode	Temp. °C	E_{imm} mV/SCE	E_{res} mV/SCE	Slop mV/min	δ µm/min	R^2
Au	20	257	179	-6.65	-	0.9800
	30	245	117	-14.60	-	0.9640
	40	212	113	-24.37	-	0.9550
	50	127	97	-17.18	-	0.9900
CoCr-alloy	20	-160	80	64.86	1.67	0.9800
	30	-180	77	64.87	1.62	0.9760
	40	-224	67	122.00	2.94	0.9680
	50	-255	60	92.78	2.17	0.9830
Mo	20	46	-48	-25.01	-	0.9899
	30	-100	-137	-6.84	-	0.9495
	40	-107	-141	-12.94	-	0.8210
	50	-112	-155	-12.70	-	0.9490
Nb	20	-310	-142	70.96	6.10	0.9100
	30	-335	-147	98.57	8.20	0.9010
	40	-361	-181	77.25	6.22	0.9640
	50	-391	-187	73.69	5.75	0.9270

Table (1) illustrated that the slopes of the straight lines had a positive sign for CoCr-alloy and Nb electrodes indicating film thickening. The rates of oxide thickening were higher for Nb electrode at all studied temperatures than that recorded for CoCr-alloy. The negative slopes recorded for Au and Mo electrodes indicated film dissolution.

The thickness of the pre immersion film formed after few seconds of dipping process (designated ḍ), was corresponding to the intercept of the linear relation of equation 3 and was found to be dependent on the type of electrode and temperature of electrolytic solution. Figure 3 illustrates the effect of temperature on ḍ and proved that at all studied temperatures, the thickness of the pre-immersion film formed on different studied electrodes follows the following descending order:

Au > Mo > CoCr-alloy > Nb.

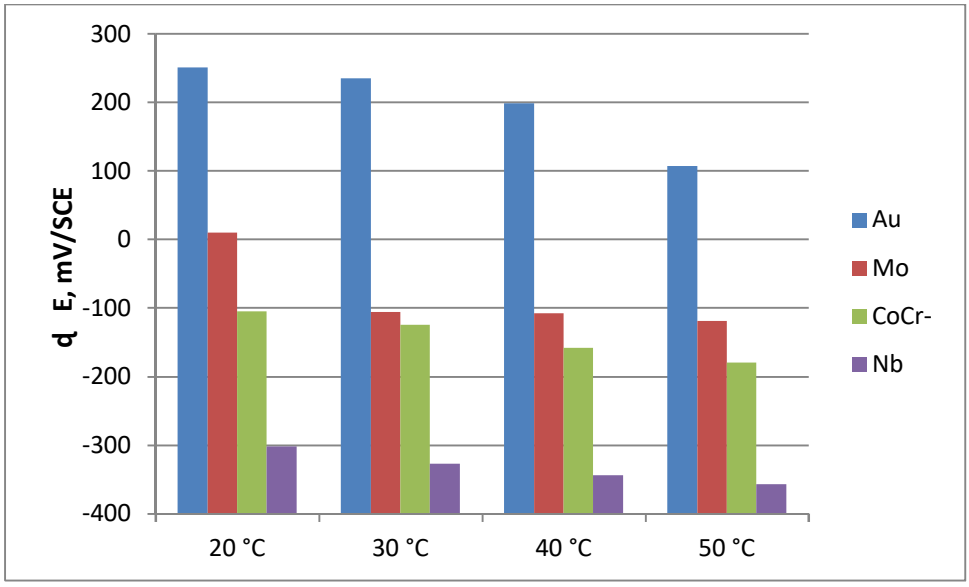

Figure 3: Effect of temperature on the pre-immersion film formed on the different studied electrodes.

Potentiodynamic measurements

Figure 4 represents the potentiodynamic scanning (PDS) plot for the four electrodes in the studied artificial saliva solution at 20°C. The study was performed at the temperature range 20 – 50°C. The PDS profiles of each electrode were nearly similar in the different studied temperatures. The CoCr-alloy, Au and Mo electrodes showed typical Tafel behavior at all temperatures. The Au electrode exhibited a lower current density in both the anodic and cathodic branches than those of CoCr-alloy and Mo electrodes. However, the anodic branches of the Nb electrode showed a little lower current density readings in the range 1000 – 1600 mV/SCE, while at 1750 mV/SCE the current density readings deviates largely to small values than that recorded for the Au electrode.

The niobium electrode exhibits a typical Tafel behavior in the cathodic region, but the anodic branch shows a deviation in current density readings out of Tafel behavior at all temperatures. The anodic current densities changed very slowly by scanning the potential in the positive direction. This indicates that its corrosion rates are in steady state *and ensured the stability of the passive* film formed on the Nb surface. This behavior was similar to that of copper in NaCl and in nitric and sulphuric acids [15-18]. In such cases, the corrosion rates and the corrosion current densities were obtained by extrapolation of the cathodic polarization curves alone to E_{corr}. The Tafel line of the cathodic polarization curve *is stretched to values behind* the corrosion potential, and then a line is made vertical to the X-axis at the corrosion potential (Figure 5). The respective potentiodynamic parameters including corrosion potential (E_{corr}), corrosion current density (I_{corr}), corrosion rate (C_R), anodic (β_a) and cathodic (β_c) Tafel slopes for the different electrodes are tabulated in Table 2.

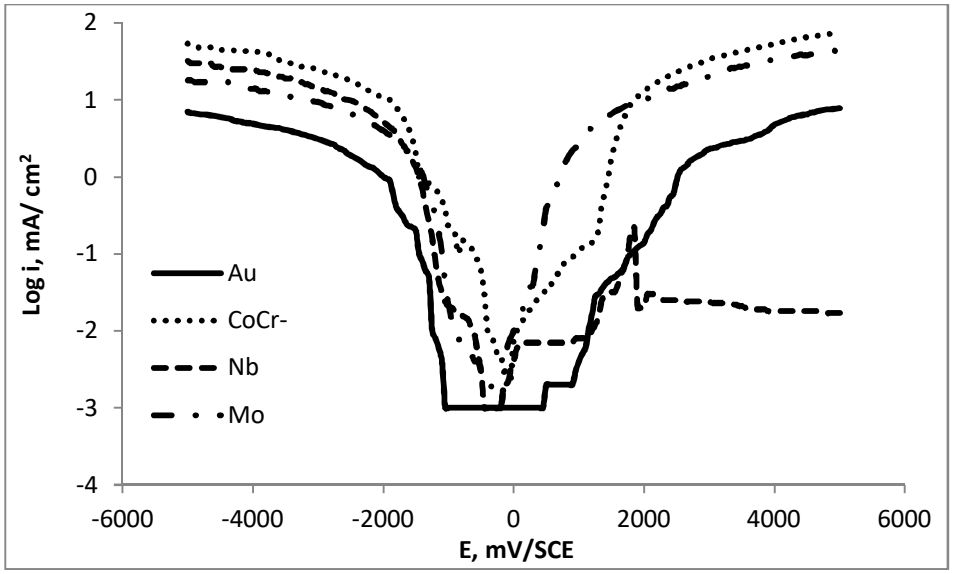

Figure 4: Potentiodynamic plot of CoCr-alloy, Nb, Mo and Au electrodes in artificial saliva solution at 20°C.

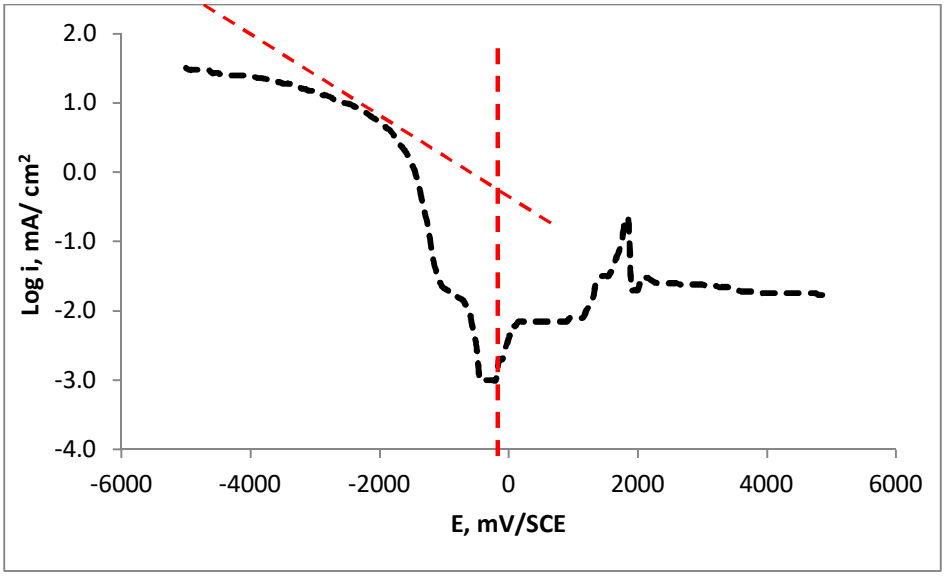

Figure 5: Tafel extrapolation of the cathodic polarization curve for Nb electrode in artificial saliva solution at 20°C.

Table 2: Potentiodynamic parameters of the four electrodes in artificial saliva solution at different temperatures

Electrode	Temp. °C	E_{corr} mV/SCE	I_{corr} mA/cm2	βc mV/dec	βa mV/dec	C_R mpy
Au	20	100	0.063	-1800	1750	6.47E-06
	30	-100	0.079	-1600	2200	8.14E-06
	40	-200	0.100	-1800	2200	1.03E-05
	50	-200	0.158	-1666	2333	1.62E-05
CoCr-alloy	20	-100	0.794	-3500	3000	2.44 E-01
	30	-100	1.259	-1600	1666	3.87 E-01
	40	-200	1.995	-1750	2000	6.14 E-01
	50	-300	3.162	-1800	2250	9.73 E-01
Mo	20	-200	0.063	-1000	750	1.27 E-02
	30	-300	0.100	-900	1000	2.02 E-02
	40	-400	0.251	-1166	1000	5.08 E-02
	50	-300	0.794	-1400	1375	1.60 E-01
Nb	20	-400	1.995	-2500	-	2.81 E-01
	30	-450	3.162	-3000	-	4.46 E-01
	40	-400	3.981	-4000	-	5.61 E-01
	50	-400	5.012	-5000	-	7.07 E-01

As a general trend, E_{corr} decrease with *increasing the temperature* for the Au and CoCr-alloy. This was the case for Mo electrode but with odd behavior at 50°C which increases to a value equal to that recorded at 30°C. Niobium electrode provides the same E_{corr} values (-400 mV/SCE) at all temperatures with one exception at 30°C (-450 mV/SCE).

It was observed from Table 2 that Au electrode had the least I_{corr} values followed by Mo electrode. The difference in current density values between the two electrodes increase with increasing temperature. At 20°C, the two electrodes provide the same I_{corr} values, while at 30, 40 and 50°C, I_{corr} increases for Mo electrode by 1.2, 2.5 and 5.0 folds respectively. This fold was very high in case of CoCr-alloy and reached to its highest values in case of Nb electrode when compared with Au electrode. The increasing I_{corr} values for CoCr-alloy *were approximately equal to* 12, 16 fold at 20, 30°C respectively and 20 fold at both 40 and 50°C. In case of Nb electrode, the increasing values were approximately equal to 31.5 fold at both 20 and 50°C, and 40 fold at both 30 and 40°C.

Relating the values of anodic and cathodic Tafel slopes with the corrosion process, it was assumed by Mansfeld [19] that, if $\beta_a > \beta_c$ means an alloy had a tendency toward passivation, while $\beta_a < \beta_c$ means an alloy had a tendency to corrode. The high values of β_a compared with the values of β_c for the Au and CoCr-alloy electrodes indicate an anodic control in the corrosion process which denotes the presence of a passive layer on the electrode surface [20].

The corrosion rates (C_R) for all electrodes, illustrated in Table 2, increased with increasing temperature. The C_R values were decreased tracking the following descending order at all temperatures: CoCr-alloy > Nb > Mo > Au. This order of passivity was not identical with that obtained for rest potential in open circuit potential measurements. The reason may be that 90 min is not a sufficient time to achieve a stable rest potential. More over the nature of the metal/solution interface was affected by the change in time and subsequently the open-circuit potential is unidentified as a characteristic of the metal [21]. Thus, open circuit potential technique is qualitative and inadequate for a full analysis [22], while potentiodynamic polarization is more sensitive and accurate technique.

The difference recorded between corrosion rates of Mo, Nb and CoCr-alloy compared with Au electrode reached its minimum values in Mo electrode which were: 1.28E-02, 2.02E-02, 5.08E-02 and 1.61E-01 at 20, 30, 40 and 50ºC respectively. The recorded differences increased with increasing temperature and reached its highest value at 50ºC. This means that under potentidynamic conditions, Au electrode can be replaced by Mo electrode at all temperatures in artificial saliva solution.

Thermodynamic considerations

The corrosion rate (C_R) is temperature dependence and can be represented by the familiar Arrhenius equation [23]:

$$\text{Log}\, C_R = A - (E_a/2.303\, RT) \qquad (5)$$

where A is a constant representing the frequency factor, E_a is the apparent activation energy of the dissolution reaction, R is the universal gas constant and T is the absolute temperature.

A plot of logarithmic variation of corrosion rates with reciprocal of absolute temperatures gave straight lines (as shown in Figure 6) with slopes of $-(E_a/2.303\, R)$.

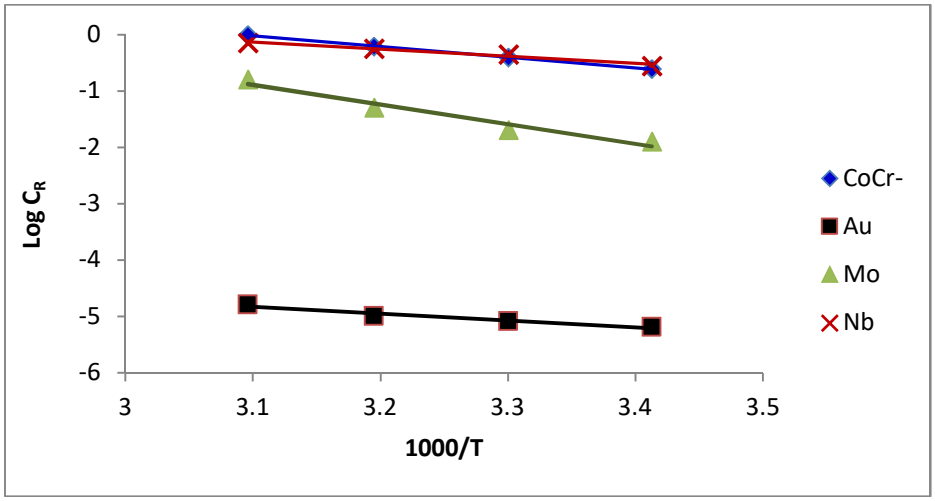

Figure 6: Arrhenius plots of the corrosion behavior of CoCr-alloy, Nb and Mo electrodes compared with Au electrode in artificial saliva solutions.

The plot illustrated that the rate of oxide film dissolution increases as the temperature increased for all electrodes. The kinetic parameters derived from Arrhenius equation including the frequency factor (A), the apparent activation energy (E_a) of the dissolution reaction and regression coefficient (R^2) are listed in Table 3.

Table 3: Activation parameters for the different electrodes in artificial saliva solutions

Electrode	A	E_a	R^2
Au	-1.0	-23.4	0.9521
CoCr-alloy	5.8	-36.2	0.9992
Mo	9.8	-66.6	0.9565
Nb	3.7	-23.7	0.9747

The higher activation energies indicate that the reaction is slow and very sensitive to temperature. Table 3 illustrated that in artificial saliva solutions, Mo had the most negative E_a value followed by CoCr-alloy, while the least negative value was recorded for Au electrode. This indicates the ease of dissolution of the passive film of Mo compared to other electrodes and the difficulty of dissolution process in case of Au electrode.

In artificial saliva solution (pH 7.8) the water molecules are involved in the cathodic reaction according to:

$$H_2O + e^- \rightarrow H + OH^- \qquad (6)$$

$$H + H \rightarrow H_2 \qquad (7)$$

The evolution of hydrogen molecules on the Mo electrode activates its surface.

The thermodynamic functions for dissolution process were obtained by applying the Eyring transition-state equation (Eq. 8) [23]:

$$\log C_R/T = \log (R/Nh) + (\Delta S/2.303R) - (\Delta H/2.303RT) \qquad (8)$$

where N is Avogadro's number, h is Planck's constant, ΔS and ΔH are the entropy and enthalpy of dissolution, respectively. Figure 7 represents a plot of $\log C_R/T$ vs. $1/T$ which gave straight lines with slopes of $[-\Delta H/2.303R]$ and intercepts of $[\log(R/Nh) + (\Delta S/2.303R)]$. The obtained values were tabulated in Table 4.

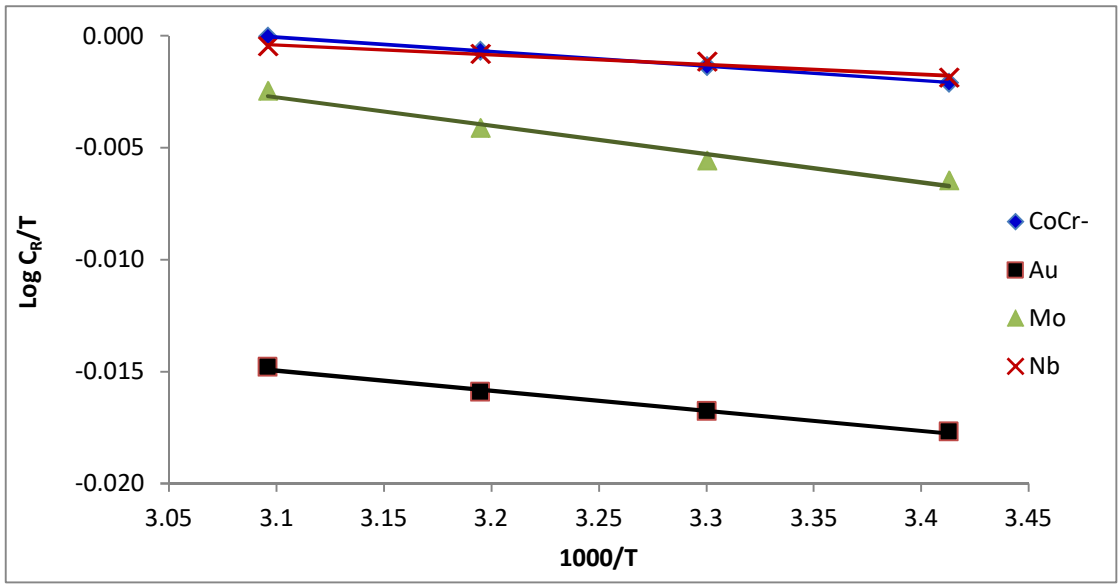

Figure 7: Transition state plots of Au, CoCr-alloy, Nb and Mo electrodes in artificial saliva solutions.

Table 4: Thermodynamic parameters for the different electrodes in artificial saliva solutions

Electrode	ΔS	ΔH	R^2
Au	-197	172	0.9926
CoCr-alloy	-197	124	1
Mo	-197	243	0.9734
Nb	-197	84	0.9703

The positive values of ΔH reflected the endothermic nature of the dissolution process which suggested the difficult and slow dissolution of electrodes in presence of artificial saliva solutions. The higher values for ΔH indicated higher protection efficiency due to the presence of an energy barrier for the reaction. Thus the electrodes surfaces adsorb the adjacent layers of solutions leading to a rise in enthalpy of the corrosion process [24, 25]. In addition, the entropy values (ΔS) for all electrodes were large and have the same negative value. This implied that the activated complex in the rate determining step represented association rather than dissociation step [11]. This reflects the formation of an ordered stable layer on the electrodes surfaces [26]. Meaning that a decrease in disordering took place on going from reactants to activated complex and the increase in the system ordering accompanied the dissolution process.

Conclusion

Open circuit potential measurements illustrated that, for each electrode, the rest potential (E_{res}) values become less noble with increasing temperature. The E_{res} for the different electrodes decreased in artificial saliva solution at all temperatures according to the following order:

Au > CoCr-alloy > Mo > Nb

From potentiodynamic polarization measurements, the niobium electrode exhibits a typical Tafel behavior in the cathodic region only at all temperatures.

The corrosion rates (C_R) for all electrodes increased with increasing temperature. The C_R values were decreased tracking the following descending order at all temperatures:

CoCr-alloy > Nb > Mo > Au

The difference recorded between corrosion rates of Mo, Nb and CoCr-alloy compared with Au electrode reached its minimum values in Mo electrode. This means that under potentidynamic conditions, Au electrode can be safely replaced by Mo electrode at all temperatures in artificial saliva solution.

REFERENCES

1- A. Preetha and R. Banerjee; Comparison of Artificial Saliva Substitutes. Trends Biomater. Artif. Organs,18(2) (2005) 178-186.
2- http://www.greenandhealthy.info/salivafightingtoothdecay.html
3- S.P. Humphrey, RDH, MSEd and R.T. Williamson, DMD, A review of saliva: Normal composition, flow, and function. J. Prosthet. Dent, 85(2) (2001) 162-169.
4- L. Joska, M. Poddana and J. Leitner; Corrosion behavior of palladium–silver–copper alloys in model saliva. Dent. Mat., 24 (2008) 1009–1016.
5- Y.J. Bai, Y.B. Wang , Y. Cheng, F. Deng, Y.F. Zheng and S.C. Wei; Comparative study on the corrosion behavior of Ti–Nb and TMA alloys for dental application in various artificial solutions. Mat. Sci. Eng., C 31 (2011) 702–711.
6- B.B. Zhang, B.L. Wang, L. Li and Y.F. Zheng; Corrosion behavior of Ti–5Ag alloy with and without thermal oxidation in artificial saliva solution. Dent. Mat., 27 (2011) 214–220.
7- M. Karthega, S. Tamilselvi and N. Rajendran; Effect of pH on the Corrosion Behaviour of Ti-6Al-4V alloy for Dental Implant Application in Fluoride Media. Trends Biomater. Artif. Organs, 20(1) (2006) 31–34.
8- D. Renita, S. Rajendran and A. Chattree; Influence of Artificial Saliva on the Corrosion Behavior of Dental Alloys: A review. Indian J. Adv. Chem. Sci., 4(4) (2016) 478-483.
9- T. Nuoh, J. Andre Mars, N. Thovhogi, D. Gihwala, A.A Baleg and M. Maaza; Influence of Temperature and pH on Corrosion Resistance of Ni-Cr and Co-Cr Dental Alloys on Oral Environmen. J. Dent. Oral Health, 22 (2015) 1–9.
10- S. Kumar and T.S.N. Sankara Narayanan; Electrochemical characterization of β-Ti alloy in Ringer's solution for implant application. J. Allo. Comp., 479 (2009) 699–703.
11- E. M. Attia, N. S. Hassan and A. M. Hyba; Corrosion Protection of Tin in 1M HCl by Expired Novacid Drug-Part I. IJAR, 4(2) (2016) 872-886.
12- A. Aladjem; Anodic oxidation of titanium and its alloys. J. Mat. Sci., 8(1973) 688 –704.
13- J.M. Abd El Kader and A.M. Shams El Din; Film thickening on nickel in aqueous solutions in relation to anions type and concentration. Br. Corros. J., 14(1979) 40 – 45.

14- F.E. Heakal, A.A. Ghoneim and A.M. Fekry; Stability of spontaneous passive films on high strength Mo-containing stainless steels in aqueous solutions. J. Appl. Electrochem., 37(2007) 405–413.
15- S. Hong, W. Chen, Y. Zhang, H.Q. Luo, M. Li and N.B. Li; Investigation of the inhibition effect of trithiocyanuric acid on corrosion of copper in 3.0 wt.% NaCl. Corros. Sci., 66 (2013) 308–314.
16- D. Wang, B. Xiang, Y. Liang, S. Song and C. Liu; Corrosion control of copper in 3.5 wt.% NaCl Solution by Domperidone: Experimental and Theoretical Study. Corros. Sci., 85 (2014) 77–86.
17- K.F. Khaled, Corrosion control of copper in nitric acid solutions using some amino acids – a combined experimental and theoretical study. Corros. Sci., 52 (2010) 3225–3234.
18- M.A. Amin, K.F. Khaled, Copper corrosion inhibition in O_2-saturated H_2SO_4 solutions. Corros. Sci., 52 (2010) 1194–1204.
19- F. Mansfeld; Electrochem. Soc., 120 (1973) 515.
20- D. Mareci, D. Sutiman, A. Cailean and G. Bolat; Comparative corrosion study of Ag–Pd and Co–Cr alloys used in dental applications. Bull. Mater. Sci, 33(4) (2010) 491–500.
21- D. Mareci, R. Chelariu, D-M Gordin, G. Ungureanu and T. Gloriant; Comparative corrosion study of Ti–Ta alloys for dental applications. Acta Biomater., 5 (2009) 3625–3639.
22- C. Manaranche, H. Hornberger; A proposal for the classification of dental alloys according to their resistance to corrosion. Dent. Mat., 23(2007) 1428–1437.
23- E.M. Attia; Dipron: an eco-friendly corrosion inhibitor for iron in HCl media in both micro and nano scale particle size - Comparative study. IJAR, 4(3) (2016) 986-1003.
24- A. Ansari, M. Znini, I. Hamdani, L. Majidi, A. Bouyanzer and B. Hammouti; Experimental and theoretical investigations anti-corrosive properties of Menthone on mild steel corrosion in hydrochloric acid. J. Mater. Environ. Sci., 5(1) (2014) 81– 94.
25- A.S. Fouda, S.A. Abdel-Maksoud and A.E. Almetwally; Corrosion inhibition of tin in sodium chloride solutions using propaneitrile derivatives. Chem. Sci. Trans., 4(1) (2015) 161–175.
26- A.M. Al-Bonayan; Corrosion inhibition of carbon steel in hydrochloric acid solution by Senna-Italica extract. IJRRAS., 22(2) (2015).